Author Manuscript

Author Manuscript

Author Manuscript

Author Manuscript

HHS Public Access

Author manuscript

Eur J Neurosci. Author manuscript; available in PMC 2023 February 23.

Published in final edited form as:

Eur J Neurosci. 2021 January ; 53(2): 416–429. doi:10.1111/ejn.14925.

Hippocampal blood–brain barrier of methamphetamine self-administering HIV-1 transgenic rats

Michael Ohene-Nyako[1,2], **Amanda L. Persons**[2,3,4], **T. Celeste Napier**[1,2,4]

[1]Department of Pharmacology, Rush University, Chicago, IL, USA

[2]Department of Physician Assistant Studies, Rush University, Chicago, IL, USA

[3]Department of Psychiatry and Behavioral Sciences, Rush University, Chicago, IL, USA

[4]Center for Compulsive Behavior and Addiction, Rush University, Chicago, IL, USA

Abstract

Combined antiretroviral therapy for HIV infection reduces plasma viral load and prolongs life. However, the brain is a viral reservoir, and pathologies such as cognitive decline and blood–brain barrier (BBB) disruption persist. Methamphetamine abuse is prevalent among HIV-infected individuals. Methamphetamine and HIV toxic proteins can disrupt the BBB, but it is unclear if there exists a common pathway by which HIV proteins and methamphetamine induce BBB damage. Also unknown are the BBB effects imposed by chronic exposure to HIV proteins in the comorbid context of chronic methamphetamine abuse. To evaluate these scenarios, we trained HIV-1 transgenic (Tg) and non-Tg rats to self-administer methamphetamine using a 21-day paradigm that produced an equivalency dose range at the low end of the amounts self-titrated by humans. Markers of BBB integrity were measured for the hippocampus, a brain region involved in cognitive function. Outcomes revealed that tight junction proteins, claudin-5 and occludin, were reduced in Tg rats independent of methamphetamine, and this co-occurred with increased levels of lipopolysaccharide, albumin (indicating barrier breakdown) and matrix metalloproteinase-9 (MMP-9; indicating barrier matrix disruption); reductions in GFAP (indicating astrocytic dysfunction); and microglial activation (indicating inflammation). Evaluations of markers for two signaling pathways that regulate MMP-9 transcription, NF-κB and ERK/ΔFosB revealed an overall genotype effect for NF-κB. Methamphetamine did not alter measurements from Tg rats, but in non-Tg rats, methamphetamine reduced occludin and GFAP,

Correspondence: T. Celeste Napier, Rush University Medical Center, 1735 W. Harrison Street, Cohn Research Building Suite #424, Chicago, IL 60612, USA. celeste_napier@rush.edu.

AUTHOR CONTRIBUTIONS

The following are the roles of the individual authors. Michael Ohene-Nyako conceived the study, acquired funding, designed the experiment, curated and analyzed the data, wrote the original draft of the manuscript, and reviewed and edited the manuscript. Amanda L Persons conceived the study, acquired funding, designed the experiment, reviewed the data and edited the original draft of the manuscript . T. Celeste Napier conceived the study, acquired funding, designed the experiment, supervised the study, wrote the original draft of the manuscript, and reviewed and edited the manuscript.

CONFLICTS OF INTEREST

The authors declare that there are no conflicts of interest.

SUPPORTING INFORMATION

Additional supporting information may be found online in the Supporting Information section.

PEER REVIEW

The peer review history for this article is available at https://publons.com/publon/10.1111/ejn.14925

Author Manuscript Author Manuscript Author Manuscript Author Manuscript

and increased MMP-9 and NF-κB. Study outcomes suggest that BBB dysregulation resulting from chronic exposure to HIV-1 proteins or methamphetamine both involve NF-κB/MMP-9.

Keywords

ERK; Fos; Iba-1; MMP; NF-κB

1 | INTRODUCTION

The blood–brain barrier (BBB) shields the brain from harmful factors carried in the circulating blood, and proper BBB structure is critical for brain health. A lattice of inter-endothelial cell tight junction proteins, for example, occludin and claudin-5, restricts paracellular movement of substances from the blood to the brain (see Daneman, 2012). As reduction or redistribution of tight junction proteins can increaseBBB permeability (Jiao, Wang, Liu, Wang, & Xue, 2011), maintenance of the paracellular lattice is an important task of numerous biochemical systems, including matrix metalloproteinases (MMPs). MMPs are endopeptidases, and the MMP-9 subtype cleaves BBB tight junction proteins such as occludin and claudin-5 (Chiu & Lai, 2013; Vermeer et al., 2009; Yang, Estrada, Thompson, Liu, & Rosenberg, 2007). An increase in MMP-9 level and/or activity is associated with a reduction in tight junction proteins and enhanced BBB permeability (Huang, Eum, Andras, Hennig, & Toborek, 2009; Northrop, Halpin, & Yamamoto, 2016). MMP-9 expression is under tight transcriptional control by several pathways, including the nuclear factor-*kappa* B (NF-κB) (Bond, Chase, Baker, & Newby, 2001) and mitogen-activated protein kinase (MAPK) pathways (Mishra, Flaga, & Kowluru, 2016). This study considered the possibility that factors which foster BBB breakdown may dysregulate MMP-9 and its upstream regulators, NF-κB and/or MAPK.

Infection with human immunodeficiency virus (HIV) increases BBB permeability (Rahimy et al., 2017) to promote infiltration of HIV-infected monocytes and macrophages into the brain (Chiodi et al., 1988; Davis et al., 1992; Resnick, Berger, Shapshak, & Tourtellotte, 1988). In infected cells, HIV-1 hijacks host machinery to transcribe viral proteins (e.g., Tat, Nef, Gp120 and Vif), some of which are released into the extracellular space and can negatively alter function of other brain cells (for review, see Arts & Hazuda, 2012). In vitro studies reveal that Tat, Nef and Gp120 reduce levels and distribution of BBB tight junction proteins to promote BBB permeability (Ju et al., 2009; Huang et al., 2014), while enhancing the level and activity of MMP-9 (Ju et al., 2009; Huang et al., 2014; Louboutin, Agrawal, Reyes, Van Bockstaele, & Strayer, 2010), MAPK pathway proteins (Toschi et al., 2006) and NF-κB (Esposito et al., 2017; Fiume et al., 2012). The extent to which in vitro studies with single viral proteins inform BBB integrity during chronic exposure to multiple HIV proteins in vivo is uncertain.

In HIV-infected individuals, abuse of psychostimulants, including methamphetamine (meth), is highly prevalent (Nerlander et al., 2018). HIV-infected meth abusers exhibit poor adherence to combined antiretroviral therapy (cART) (Hinkin et al., 2007) and suffer more severe neuropathology than non-abusers (Soontornniyomkij et al., 2016). Meth disrupts the

Author Manuscript Author Manuscript Author Manuscript Author Manuscript

BBB in vivo (Eugenin, Greco, Frases, Nosanchuk, & Martinez, 2013; Kousik, Napier, & Carvey, 2012; Northrop et al., 2016) and alters transcription regulators of MMP-9 such as NF-κB and MAPK signaling in vitro (Zhang et al., 2015). Taken together, the above suggest that meth may worsen BBB pathology induced by HIV proteins.

Whether the pathways that are engaged by HIV proteins and by meth to regulate BBB function are in common (potentially additive) or converge (potentially synergistic) is unclear. To make this determination, we evaluated the BBB in the hippocampus, a brain region vulnerable to HIV infection (Castelo, Sherman, Courtney, Melrose, & Stern, 2006; Maki et al., 2009) and meth (Choi et al., 2018). We hypothesized that exposure to HIV-1 proteins in vivo will impair the BBB and that the pathology will be enhanced in the comorbid brain state. We utilized HIV-1 transgenic (Tg) rats that chronically express seven of the nine HIV-1 proteins. The HIV-1 transgenic rat model recapitulates several aspects of the central nervous system (CNS) pathologies experienced by HIV-infected individuals and is considered to be a useful model for studying neuroAIDS (Lee et al., 2014; Lentz et al., 2014; Repunte-Canonigo et al., 2014). The HIV-1 transgenic rat model is also thought to model HIV-infected patients on cART (Peng et al., 2010), wherein viral titers in the serum are negligible but viral reservoirs persist, such as those of the brain. Using meth self-administering HIV-1 Tg rats, we show that occludin and claudin-5 are decreased by chronic exposure to HIV proteins, and meth reduced occludin. Increased levels of lipopolysaccharide and albumin indicated barrier breakdown. The impairments were associated with increased MMP-9 levels and NF-kB activation.

2 | MATERIALS AND METHODS

2.1 | Animals

Rat brain tissues were obtained from a specimen repository in the laboratory of Dr. T. Celeste Napier (Rush University Medical Center). The brains were harvested from 20 male HIV-1 Tg (17–22 weeks old) and 20 sex- and age-matched non-Tg Fischer 344 rats. Information regarding animal care and self-administration procedures is published elsewhere (Persons et al., 2018). Briefly, rats purchased from Envigo Laboratories were housed in genotype- and treatment-similar pairs in the Rush University vivarium. Food and water were provided ad libitum throughout the study. All procedures performed were in accordance with the Guide for the Care and Use of Laboratory Animals (National Research Council) and as approved by the Rush University Institutional Animal Care and Use Committee.

2.2 | Intravenous catheter implantation for self-administration

Rats received intravenous drugs through custom-made silastic catheters (0.3 mm ID × 0.64 mm OD; Dow Corning Co.) inserted into their right jugular vein. The distal end of the catheters extended subcutaneously over the mid-scapular region and exited through a metal guide cannula (22 gauge; Plastics One Inc.) anchored to a subcutaneously implanted vinyl mesh. Duration of recovery post-surgery was 10–14 days. Catheters were flushed daily with 0.1–0.2 ml sterile saline to maintain patency.

Author Manuscript Author Manuscript Author Manuscript Author Manuscript

2.3 | Self-administration

Rats were trained to self-administer meth in operant chambers equipped with two "nose-poke" holes, a stimulus light above each hole, an audio tone generator and a house light. Nose-poking is an ethologically relevant behavior and a commonly employed operant task with rodents (e.g., Brown et al., 2020; Chen et al., 2020; Fredriksson et al., 2019; Gordon-Fennell et al., 2019; Hong, Kang, Chen, & Choi, 2019; Oliva & Wanat, 2019). Each operant chamber was enclosed in a ventilated, sound-attenuating chamber. Infusions were delivered via syringes in a motor-driven pump. (+)-meth HCl (Sigma-Aldrich) was dissolved in sterile saline for the self-administration operant task.

Operant sessions were conducted 2 hr/day for a total of 21 days. On test days 1–7, a nose-poke in the active hole resulted in a 6-s infusion of meth (0.02 mg/kg/0.05 ml) on a fixed ratio 1 (FR1) schedule of reinforcement. There was no post-infusion timeout period. For test days 8–21, the dose of meth was increased to 0.04 mg/kg per 0.05-ml infusion. Nose-pokes in the inactive hole had no programmed consequence. Control rats were saline-yoked to a meth counterpart of the same genotype. The yoked rats received a non-contingent infusion of saline (0.05 ml) each time their meth counterpart received a meth infusion. For saline-yoked rats, nose-pokes in either hole were recorded but had no programmed consequence.

Brain tissues were harvested one day following the operant task and hemisected. The left hemisphere of the brain was dissected and fast-frozen for immunoblotting. The right hemisphere was immersion-fixed in 4% paraformaldehyde overnight followed by preservation in sucrose (30%). The hemispheres were then sliced into serial coronal sections (40 μm) using a sliding microtome and stored in a cryoprotectant at −20°C for immunohistochemistry.

2.4 | Immunoblotting

Immunoblotting followed our previously published protocols (Herrold et al., 2009; Kousik, Carvey, & Napier, 2014; Ohene-Nyako, Persons, & Napier, 2018; Persons et al., 2018) with minor modifications. Briefly, fast-frozen hippocampal samples were homogenized in ice-cold lysis buffer [containing in mM: 25 HEPES (pH 7.4.), 2 EDTA, 500 NaCl, 20 NaF, 1 PMSF, 1 DTT, 0.1% v/v nonidet P-40, 1× HALT protease inhibitor cocktail (Thermo Fisher), 1× phosphatase inhibitor cocktails II and III (Sigma-Aldrich)]. The homogenate was centrifuged at 20854 *g* for 2min at 4°C, sonicated for 5 s and centrifuged again, and the supernatant was aliquoted and stored at −80°C. Protein concentration was determined by Bradford assay (Bradford, 1976). Samples (40 μg) were electrophoresed on 10% Tris-HCl gels and transferred to nitrocellulose membranes. Non-specific binding sites were blocked using Odyssey blocking buffer (LI-COR) for 1h at room temperature (RT). Membranes were incubated overnight at 4°C with primary antibodies: occludin (1:250, #33–1500 EMD Millipore), claudin-5 (1:500, #35–2500 EMD Millipore), MMP-9 (1:500, #NBP2–13173 Novus Biologicals), albumin (1:500, #NBP1–32458 Novus Biologicals), extracellular signal-regulated kinase, pERK/ERK (1:1,000, #9101/9102 Cell Signaling Technology), delta (Δ)FosB (1:1,000, #9205 Cell Signaling Technology) and pNF-kB/NF-kB (1:500, #3033/8242 Cell Signaling Technology). After washing in Tris-buffered saline⁄Tween-20

Author Manuscript Author Manuscript Author Manuscript Author Manuscript

(TBS-T; 20 mM Tris, 137mM NaCl, 0.5% Tween-20, pH 7.4), membranes were incubated in IR dye-conjugated goat anti-rabbit secondary antibody (1:5,000. #925–32211, LI-COR) or goat anti-mouse secondary antibody (1:5,000. #925–32210, LI-COR) for 1h at RT. Revert Total Protein Stain (#926–11010, LI-COR) was used to assess loading. Membranes were scanned with a LI-COR image scanner, and optical density was determined using LI-COR Image Studio Lite (V5.2). Antibody verification was performed using orthogonal and/or independent antibody tests described by Uhlen et al. (2016).

2.5 | Immunohistochemistry (IHC)

Free-floating coronal sections (40 μm) containing the hippocampus were washed in dilution media (TBS with 0.05% Triton X-100) to remove cryoprotectant. Endogenous peroxidases were blocked using 2.13% sodium periodate (Sigma-Aldrich) in TBS for 20min followed by washes in dilution media. Sections were blocked for 1h in a solution containing dilution media, 6% v/v normal species-specific serum (Thermo Fisher) and 2% w/v bovine serum albumin (BSA). Following blocking, sections were incubated with Iba-1 (1:200, #019–19741 WAKO) or GFAP (1:500, #3670S Cell Signaling Technology) antibodies overnight at RT. Primary antibody diluent contained 0.05M PBS, 1% v/v normal serum (Thermo Fisher), 1%w/v BSA and 0.04% v/v Triton X-100. Tissues were washed in dilution media and incubated for 1h in biotinylated goat anti-rabbit secondary antibody (for Iba-1) (1:500, #BA-1000 Vector Laboratories, Inc.) or horse anti-mouse secondary antibody (for GFAP) (1:200, #BA-2000 Vector Laboratories, Inc.). Iba-1 and GFAP immunoreactivity (ir) were visualized using a peroxidase-conjugated avidin–biotin complex (Vector Laboratories, Inc.) and 3, 3-diaminobenzidine in three subfields of the hippocampus (i.e., the CA1, CA3 and DG). Pathology within these 3 subfields negatively correlates with an impairment in the generation and recall of episodic memory (Mueller, Chao, Berman, & Weiner, 2011), a hippocampal impairment experienced by HIV-infected individuals (Castelo et al., 2006; Maki et al., 2009). A primary omit control was also conducted. Optical density analysis was performed on 4× GFAP-stained images using ImageJ software (NIH). All analyses were performed by a treatment- and genotype-blinded observer using hippocampal photomicrographs taken from bregma −4.08 mm to −4.36 mm (Paxinos & Watson, 2009).

2.6 | CellProfiler analysis of Iba-1-stained microglial morphology

Cell body and cell sizes of Iba-1-stained microglia were measured and quantified using CellProfiler v3.1.8 (BROAD Institute) (see Figure 1a). Briefly, 40× images of Iba-1-stained microglia were converted to 8-bit grayscale images and uploaded into the CellProfiler software. Using the measuring tool in CellProfiler, the soma diameter and length of the smallest and largest microglial cells were determined. A CellProfiler pipeline for analyzing microglia (pipeline and detailed instructions can be obtained from Bloomfield et al., 2018) was downloaded and opened in the CellProfiler software. The microglial analysis pipeline was then modified by inserting the dimensions of the smallest and largest measured cell parameters (the smallest and largest soma diameter and area occupied by cell) into their respective windows in the CellProfiler software. A test run was initiated to validate the identified objects followed by an initiation of a full automated run. The total area occupied by each microglial cell (soma and processes) and the area of its corresponding soma are computed by the CellProfiler software. An average soma size and cell size were then

Author Manuscript Author Manuscript Author Manuscript Author Manuscript

computed for each uploaded section and analyzed as a ratio of the two variables (soma size (cell body) to cell size).

2.7 | ELISA

We previously showed colon barrier permeability in the HIV-1 Tg rats (Persons et al., 2018). Hence, in addition to immunoblot evaluations of hippocampal albumin levels as an indirect measure of an impaired BBB function, we also evaluated lipopolysaccharide (LPS) concentrations. Hippocampal LPS was determined using the Pierce Limulus Amebocyte Lysate (LAL) Chromogenic Endotoxin Quantification Kit (#88282, Thermo Fisher). The kit contained purified endotoxin standards, endotoxin-free water, amebocyte lysate reagent and a chromogenic substrate. All materials for the LPS assay were certified endotoxin-free. Hippocampal homogenates, blanks and endotoxin standards were incubated with amebocyte lysate reagent at a 1:1 ratio in a 96-well plate for 14 min at 37°C. A 100 μl prewarmed solution of chromogenic substrate was added to each well and incubated for 6 min. A stop reagent made up of 25% acetic acid in endotoxin-free water was added to each well after the 6-min incubation. Absorbance of end products was measured at 405 nm in a spectrophotometer (SpectraMax Plus model 384, Molecular Devices). LPS levels (in EU/ml) were generated based on extrapolations from the standard endotoxin curve.

2.8 | Data analyses

All data were standardized as % control, that is, the saline-yoked non-Tg group. ERK and NF-κB data are presented as a ratio of activated (p) to total proteins. Iba-1 data are presented as a ratio of cell body to cell size (Hovens et al., 2014). Data from immunoblots, IHC and ELISA were analyzed using a two-way ANOVA followed by a *post hoc* Newman–Keuls test. A significant interaction by two-way ANOVA was used to indicate synergy. Planned contrasts selected for comparisons were (a) treatment effects within each genotype and (b) treatment effects between each genotype. Pearson's correlation was used to determine the relationship between claudin-5 levels and LPS levels and between claudin-5 and MMP-9 levels. All statistical analyses were performed using GraphPad Prism software v 6.0, with significance set at $p < .05$. Data are presented as mean + *SEM* or mean ± *SEM*.

2.9 | Scientific Rigor

To enhance rigor and reduce experimenter bias, data were analyzed by a genotype-blinded observer. Immunoblotting and ELISAs were performed with positive control samples. In the event where a positive control was not available, immunoblotting bands were verified by an "independent antibody validation test" or an "orthogonal test" as proposed by Uhlen and colleagues (Uhlen et al., 2016).

3 | RESULTS

3.1 | Meth self-administration

As previously reported (Persons et al., 2018), the average daily meth self-administered by the Tg and non-Tg rats was 0.21 mg/kg (Tg) and 0.25 mg/kg (non-Tg), respectively, which converts to a human equivalence of ~0.1 mg/kg (Nair & Jacob, 2016). This falls within the lower end of the range of meth (i.e., 0.17–0.70 mg/kg) taken by humans during recreational

Author Manuscript Author Manuscript Author Manuscript Author Manuscript

use (e.g., Kirkpatrick et al., 2012; Melega, Cho, Harvey, & Lacan, 2007). There was no difference between genotypes with respect to meth intake (t_{17} = 1.38, p = .20).

3.2 | Blood–brain barrier integrity

BBB integrity was assessed by measuring hippocampal levels of tight junction proteins and the presence of a circulating gut-derived factor, LPS, that is not present in brains with an intact BBB. As illustrated in Figure 1, hippocampal levels of occludin demonstrated a significant main effect for genotype ($F_{1,29}$ = 11.16, p = .002) with no treatment main effect ($F_{1,29}$ = 3.40, p = .08) and no interaction ($F_{1,29}$ = 2.31, p = .14). A significant main effect for genotype was also observed for hippocampal claudin-5 levels ($F_{1,30}$ = 6.18, p = .02) with no treatment main effect ($F_{1,30}$ = 3.53, p = .07) and no interaction ($F_{1,30}$ = 0.41, p = .53). Consistent with the genotype main effect, *post hoc* analysis for occludin revealed a significant difference between saline-yoked Tg and saline-yoked non-Tg rats. Differences were also observed between non-Tg rats that self-administered meth and saline-yoked non-Tg rats, verifying that the amount of self-administered meth was sufficient to alter occludin levels in the absence of HIV-1 proteins. For claudin-5, *post hoc* analysis did not reveal differences between any of the planned contrasts. Similar outcomes for the transgenic and meth effect on occludin were observed in ventral striatal tissues of meth self-administering Tg and non-Tg rats (see Figure S2).

LPS levels demonstrated a significant main effect for genotype ($F_{1,19}$ = 27.85, p < .0001) but no treatment main effect ($F_{1,19}$ = 0.004, p = .95) or interaction ($F_{1,19}$ = 0.01, p = .94) (Figure 2a). *Post hoc* analysis revealed significant differences between saline-yoked Tg and saline-yoked non-Tg rats, and between meth Tg and meth non-Tg rats. Consistent with the outcomes of the LPS, a genotype main effect was observed for albumin levels ($F_{1,29}$ = 20.41, p < .0001) but no treatment main effect ($F_{1,29}$ = 2.92, p = .098) or interaction ($F_{1,29}$ = 1.88, p = .18) (Figure 2b). *Post hoc* analysis revealed significant differences between saline-yoked Tg and saline-yoked non-Tg rats, and between meth non-Tg and saline-yoked non-Tg rats. LPS levels negatively correlated with hippocampal claudin-5 (r = −0.75, p = .02) and occludin (r = −0.56, p = .04) (Figure 3a,b), and albumin levels negatively correlated with hippocampal occludin (r = −0.69, p = .007) (Figure 3c) levels in Tg rats (pooled across treatments).

3.3 | Iba-1 and GFAP IHC

As an index of inflammation, the relative size of Iba-1-stained somata and levels of GFAP staining were quantified in three subfields of the hippocampus (i.e., the CA1, CA3 and DG). For Iba-1, a significant genotype effect was observed for all evaluated subfields (CA1: $F_{1,27}$ = 66.03, p < .0001; CA3: $F_{1,27}$ = 27.85, p < .0001; and DG: $F_{1,27}$ = 18.44, p = .0003). There were no treatment effects (CA1: $F_{1,27}$ = 0.06, p = .80; CA3: $F_{1,27}$ = 0.20, p = .19; and DG: $F_{1,27}$ = 1.46, p = .24) or interaction (CA1: $F_{1,27}$ = 0.01, p = .92; CA3: $F_{1,27}$ = 0.42, p = .53; and DG: $F_{1,27}$ = 0.31, p = .58) (Figure 4). Consistent with the genotype main effect, *post hoc* analysis revealed significant differences (p < .05) between saline-yoked Tg and saline-yoked non-Tg rats, and between meth Tg and meth non-Tg rats for all subfields evaluated.

Author Manuscript Author Manuscript Author Manuscript Author Manuscript

GFAP immunohistochemical staining demonstrated a significant genotype effect in all subfields (CA1: $F_{1,25} = 5.49$, $p = .03$; CA3: $F_{1,25} = 27.85$, $p < .0001$; and DG: $F_{1, 25} = 5.92$, $p = .03$). A significant treatment effect was observed for DG and CA3 subfields (CA3: $F_{1,25} = 9.16$, $p = .007$ and DG: $F_{1,25} = 8.74$, $p = .007$) but not CA1 (CA1; $F_{1,25} = 2.33$, $p = .14$). There were no significant interactions (CA1; $F_{1,25} = 2.35$, $p = .14$, CA3; $F_{1,25} = 2.40$, $p = .14$ and DG; $F_{1,25} = 2.01$, $p = .1$) (Figure 5). Consistent with the genotype and treatment main effects, *post hoc* analysis revealed significant differences ($p < .05$) between saline-yoked Tg and saline-yoked non-Tg rats, and between saline-yoked non-Tg and meth non-Tg rats for all subfields evaluated. There were no observable differences in astroglial morphology in any of the treatment groups.

3.4 | MMP-9 and MMP-9 transcription regulators

We evaluated MMP-9 level and transcription regulators in the hippocampus of meth self-administering Tg and non-Tg rats. Two-way ANOVA revealed a significant genotype effect for MMP-9 protein levels ($F_{1,26} = 14.84$, $p = .0007$) but no treatment main effect ($F_{1,26} = 3.76$, $p = .06$) or interaction ($F_{1,26} = 1.25$, $p = .27$) (Figure 6). Consistent with the genotype main effect, *post hoc* analysis revealed significant differences between saline-yoked Tg and saline-yoked non-Tg rats. There was also a significant difference between meth non-Tg and saline-yoked non-Tg rats. Pearson's correlation revealed an inverse relationship between claudin-5 level in HIV-1 Tg rats (pooled across treatments) and MMP-9 level ($r = 0.71$, $p = .004$) (Figure 6).

Evaluation of two upstream signaling pathways that regulate MMP-9 revealed no differences in pERK/ERK or ΔFosB (Figure 7). A significant genotype effect for pNF-κB/NF-κB protein levels was observed ($F_{1,29} = 11.97$, $p = .002$) with no treatment main effect ($F_{1,29} = 2.83$, $p = .10$) or interaction ($F_{1,29} = 1.33$, $p = .26$) (Figure 7). Consistent with the genotype main effect, *post hoc* analysis revealed significant differences ($p < .05$) between saline-yoked Tg and saline-yoked non-Tg rats, and between meth non-Tg and saline-yoked non-Tg rats. There was also a significant difference between meth Tg rats and saline-yoked non-Tg rats.

4 | DISCUSSION

The current study evaluated BBB integrity using HIV-1 Tg rats, which modeled aspects of HIV-associated pathology in cART-treated humans; meth self-administration modeled the self-titration features of humans that abuse meth. Outcomes demonstrated that exposure to HIV proteins impaired BBB integrity, increased brain infiltration of peripheral contents that are excluded by an intact BBB, and promoted activation of microglial cells. The BBB effects of meth self-administration involved a reduction in occludin. MMP-9 and MMP-9-regulating proteins were increased independently by HIV-1 proteins and by meth. Overall, the results demonstrate that HIV-1 proteins and meth disrupt hippocampal BBB and that a dysregulation in MMP-9 signaling may be involved.

The finding that chronic exposure to HIV-1 proteins reduced levels of occludin and claudin-5 recapitulates observations from HIV-1-infected humans (Rahimy et al., 2017) and complements observations from in vitro studies and in vivo studies wherein single HIV-1

Author Manuscript Author Manuscript Author Manuscript Author Manuscript

proteins are investigated (Andras et al., 2003, 2005; Kanmogne, Primeaux, & Grammas, 2005; Xu et al., 2012). We previously demonstrated colon barrier permeability in HIV-1 Tg rats (Persons et al., 2018) which would allow the translocation of bacteria (e.g., LPS) from the colon into the systemic circulation. Indicating that the BBB is also impaired in Tg rats, this gut-derived substance infiltrated the hippocampus in Tg rats. LPS activates immune cells such as microglia (Hoogland et al., 2018) resulting in the release of pro-inflammatory cytokines such as TNF-α and IFN-γ (Lively & Schlichter, 2018). These cytokines activate post-synaptic receptors to increase the transcription of pro-inflammatory mediators and endopeptidases such as metalloproteinases (He, 1996), which degrade BBB junction proteins. While LPS infiltration may explain the microglial activation observed in the current study, it is also possible that HIV-1 proteins in the brains of Tg rats may have contributed to the observed microglial activation. In either case, chronic maladaptive activation of microglia is detrimental to the BBB. By increasing central nervous system inflammation, LPS can also enhance neuropathology (e.g., see Lull & Block, 2010). The concept of gut pathology affecting brain outcomes is described for humans with colon barrier pathology; for example, cerebral vasculitis and neuropathology are reported in patients with Crohn's disease (Gobbele, Reith, & Block, 2000). The current LPS outcomes therefore provide an example of how gut pathology may influence the progression of brain pathology in the context of HIV protein exposure.

The LPS outcomes were corroborated by the findings that albumin levels were also elevated in the hippocampus of meth self-administering HIV-1 Tg and non-Tg rats, thus providing converging evidence of functional impairment to the BBB. Albumin synthesis occurs in the liver after which the protein is transported into the bloodstream (Moman, Gupta, Sheikh, & Varacallo, 2020). Albumin plays a vital role in regulating and maintaining the oncotic pressure of blood (Moman et al., 2020). CNS albumin infiltration occurs when the BBB is damaged or impaired. Hence, CNS and/or cerebrospinal fluid albumin levels are commonly used as an indicator of BBB pathology (e.g., Abdulle, Hagberg, & Gisslén, 2005; Anesten et al., 2016; Farhadian et al., 2019; Rahimy et al., 2017). The observed Tg effects on albumin infiltration recapitulate observations from cART-treated HIV-infected individuals who have attained negligible serum viral titer (Rahimy et al., 2017). This suggests that viral proteins expressed in CNS reservoirs may account in part for the BBB pathology experienced by virally suppressed HIV-infected individuals. Interestingly, the low dose of self-titrated meth also increased hippocampal albumin infiltration in the non-Tg rats. This observation corroborates our previous report (Kousik, Graves, Napier, Zhao, & Carvey, 2011) and other investigators (e.g., Eugenin et al., 2013; Northrop et al., 2016) showing meth-induced BBB dysregulation. It is also known that meth increases extracellular matrix-degrading enzymes such as MMP-9 to degrade the BBB (Northrop et al., 2016). In these studies, meth was administered acutely at relatively higher doses. The outcomes of the present study reveal that chronic exposure to low, physiologically relevant doses of meth has detrimental effects on the BBB integrity and this is associated with elevated MMP-9.

Reported effects of meth on the BBB are inconsistent and likely reflect differences in models, outcome measures and meth treatment protocols, including doses; acute, repeated or chronic treatments; and contingent or non-contingent administration. For example, BBB permeability to albumin and/or FITC-labeled albumin was observed in the current study and

Author Manuscript Author Manuscript Author Manuscript Author Manuscript

reported in rats injected intraperitoneally with 3 mg/kg meth (Kousik et al., 2011). Contrary to these observations, a study using lucifer yellow showed no functional permeability to the BBB with moderate concentrations of meth in vitro, despite reductions in ZO-1 levels (Patel et al., 2017). Such variation in observed functional outcomes may be due to differences in the type of functional assay used and the degree of BBB damage induced by meth. Albumin has a molecular weight of ~60–67 kDa, while the molecular weight of lucifer yellow is ~0.5 kDa. BBB infiltration of smaller molecular weight compounds such as lucifer yellow is indicative of minimal BBB impairment (i.e., restricted to paracellular barriers), while infiltration of larger molecular weight compounds (≥66 kDa) could indicate a greater BBB pathology (i.e., both paracellular and transcellular permeability) (Muradashvili et al., 2012). In the current study, no effects of meth were observed for levels of hippocampal LPS, which has a molecular weight range of 50–100 kDa, despite the elevations of albumin. This indicates that the BBB was able to restrict the relatively large LPS molecules while relatively lower molecular weight compounds like albumin infiltrated a partially impaired BBB. Taken together, these observations indicate that both HIV-1 proteins and meth can damage aspects of the BBB and that chronic exposure to HIV-1 proteins induces greater permeability than that imposed by self-administered meth.

BBB permeability enhances brain inflammation, and this can be indicated by the morphology of microglia. Resting microglia assume a ramified morphology with small soma and thin, long projections or ramifications; activated microglia assume an amoeboid morphology with retracted processes (see Crews & Vetreno, 2016). The HIV-1 Tg rats exhibited increased microglial activation in all evaluated subfields of the hippocampus. This observation recapitulated the observation of Reid and colleagues who reported mild activation of microglia in the Tg rat brain (Reid et al., 2016). The observed increase in microglial activation by the HIV-1 Tg state paralleled the enhancement in LPS levels. As LPS increases brain inflammation (Lull & Block, 2010), the observed increase in microglial activation may be due in part to the infiltrating LPS because of the impaired BBB.

GFAP is an intermediary filament expressed by astrocytic cells. Astrocytic cells extend their foot processes to the BBB to reinforce the barrier, and astrocytic dysregulation is associated with an impaired BBB (Watkins et al., 2014). Thus, as a marker of astrocytes, dysregulation of GFAP may indicate astrocytic dysfunction. In the current study, GFAP immunoreactivity was decreased in all evaluated subfields of the hippocampus in HIV-1 Tg rats. This observation recapitulates the observations of Reid and colleagues who reported a reduction in GFAP immunoreactivity in the cortex, striatum and hippocampus of HIV-1 Tg rats (Reid et al., 2016). It is, however, uncertain whether the reduction in GFAP immunoreactivity reflects a reduction in astroglial cell numbers or protein level. GFAP protein level can decrease when GFAP-expressing cells are exposed to stressors such as mild increases in temperature (Sugaya-Fukasawa, Watanabe, Tamura, Egashira, & Hisatomi, 2011). LPS observed in the hippocampus of HIV-1 Tg rats is a pyrogen (Kozak, Conn, & Kluger, 1994). Thus, alteration in temperature (whether transient or chronic) may account in part for the observed reduction in GFAP immunoreactivity. GFAP-positive glia are particularly important in maintaining barrier integrity, and destruction of GFAP-positive enteric glia is associated with an increase in epithelial barrier permeability (e.g., see Gulbransen & Sharkey, 2012; Yu & Li, 2014). It is therefore likely that the reduction in GFAP levels seen

Author Manuscript Author Manuscript Author Manuscript Author Manuscript

in the current study may also reflect a dysfunction in astroglia cells within the brain of the HIV-1 Tg rats which may perpetuate BBB pathology.

To help elucidate possible mediators of the BBB pathology, we evaluated hippocampal levels of MMP-9 and upstream transcription regulators. HIV-1 Tat increases MMP-9 in in vitro models of the BBB (Ju et al., 2009) and in HIV-infected monocytes (Huang et al., 2009). Data from the current study confirm these in vitro findings, for MMP-9, were increased in the hippocampus of Tg rats and levels negatively correlated with tight junction protein levels consistent with a possible role for MMP-9 in BBB pathology. Recapitulating the observation of Northrop and colleagues (Northrop et al., 2016), the low dose of self-administered meth was sufficient to increase MMP-9 levels in non-Tg rats. These rats also showed a reduction in hippocampal occludin, further supporting a role of MMP-9 in the BBB pathology induced by meth exposure.

To better understand the possible mechanism underlying the HIV protein and meth-induced increases in MMP-9, we evaluated transcription regulators of MMP-9. ERK and ΔFosB were not changed by genotype or treatment in the hippocampus. These observations contradict our previous observation in the nucleus accumbens where ERK, ΔFosB and dopamine D1 receptor (D1R) immunoreactivity were increased in the nucleus accumbens of meth self-administering HIV-1 Tg rats (Ohene-Nyako et al., 2018). D1R is a stimulatory G protein-coupled receptor that increases ERK activation (Valjent et al., 2005). High densities of D1Rs are localized in the nucleus accumbens (Dawson, Gehlert, McCabe, Barnett, & Wamsley, 1986), whereas the hippocampus exhibits low D1R expression (Dawson et al., 1986). Thus, differences in D1R distribution may explain the variation in pERK/ERK outcomes between the current study and our previous study (Ohene-Nyako et al., 2018). Another transcription regulator of MMP-9, pNF-κB, was increased in the hippocampus of Tg rats. This observation is similar to that obtained with in vitro studies using human brain microvascular endothelial cells (Huang et al., 2009) and astrocytic cells (Ju et al., 2009) treated with Tat or HIV-infected monocytes. Two signaling pathways regulate the activation of NF-κB. These pathways are known as the canonical and non-canonical NF-κB pathways. The canonical pathway of NF-κB activation involves activation of TNF-α receptors or members of the Toll-like receptor (TLR) superfamily. The HIV-1 protein Tat directly interacts with the TLR subtype 4 (TLR4) to increase production of TNF-α (Ben, Leghmari, Planes, Thieblemont, & Bahraoui, 2013). One of the downstream signaling proteins activated by the TLR4 and TNF-α pathway is NF-κB (El-Hage et al., 2008), for example, exposure to HIV-1 Tat increases both TNF-α levels and NF-κB activation in vitro (El-Hage et al., 2008). Tat interacts with NF-κB and IκBα to increase activation and nuclear translocation of NF-κB (Fiume et al., 2012). Thus, activation of TNF-α, TLRs or a direct interaction of HIV proteins and NF-κB may underlie the increase in NF-κB activation seen in Tg rats. Meth also increased NF-κB activation in non-Tg rats. This observation complements the observation of Zhang and colleagues who showed a meth-induced increase in NF-κB activation in cultured astrocytic cells (Zhang et al., 2015). Meth increases TNF-α receptor expression (Park et al., 2017) and activates TLR4 (Wang et al., 2019). These actions of meth may underlie the increased NF-κB activation observed in the non-Tg rats. Taken together, HIV proteins and meth independently increased MMP-9 possibly through NF-κB activation but not MAPK activation.

Author Manuscript Author Manuscript Author Manuscript Author Manuscript

While HIV-1 proteins and meth alter NF-κB and MMP-9 via common signaling pathways (e.g., interaction with TLR4 to increase NF-κB activation), some HIV-1 proteins can also directly activate NF-κB, that is, *via* direct interaction of Tat with NF-κB and IκBα to increase NF-κB activation (Fiume et al., 2012). Thus, the effects of HIV-1 protein exposure and meth on the BBB could be additive or synergistic. In the current study, no synergy or additivity was observed between the HIV-1 transgenic state and meth. However, there were trends for meth to potentiate the effects of HIV-1 proteins on claudin-5 and MMP-9 levels in the comorbid brain. The doses of meth self-administered by the HIV-1 Tg rats and non-Tg rats in the current study were very low compared to doses administered by other rat strains (e.g., Sprague Dawley and Lewis rats (Graves, Clark, Traynor, Hu, & Napier, 2015; Kruzich & Xi, 2006)). The low self-administered doses may explain the lack of observable interaction between the transgenic state and meth. This notwithstanding, the low meth doses were sufficient to decrease occludin and increase MMP-9 protein level in the non-Tg rats, suggesting that a significant HIV-Tg-meth interaction may be apparent with relatively higher doses of meth. Furthermore, the HIV-1 Tg rat model consistently expresses HIV-1 proteins depicting highly active reservoirs in the brains of infected individuals. As a result, the effects of the HIV transgenic state may have been sufficiently robust in the HIV-1 Tg rats to mask the effects of meth on the evaluated outcomes. It is possible that in the event where viral reservoirs are partially active and/or when meth doses are sufficiently high, a significant interaction between HIV-1 proteins and meth will be apparent.

In conclusion, this study provides critical information regarding the effects of HIV proteins and meth on the BBB in vivo. The alterations in markers that mediate the pathophysiological remodeling of the BBB by chronic exposure to HIV-1 proteins and meth may explain the persistent BBB dysregulation in infected patients and meth abusers.

Supplementary Material

Refer to Web version on PubMed Central for supplementary material.

ACKNOWLEDGEMENTS

This study was funded by the National Institutes of Health grant P30A1082151 and a R25MH080661 subaward grant from the Johns Hopkins University.

Funding information

National Institute of Mental Health, Grant/Award Number: R25MH080661; National Institutes of Health, Grant/Award Number: P30A1082151; Johns Hopkins University

DATA AVAILABILITY STATEMENT

The authors confirm that all data pertaining to this manuscript are available and will be shared with the scientific community upon request.

Abbreviations:

ΔFosB	Delta FosB

Author Manuscript Author Manuscript Author Manuscript Author Manuscript

BBB	Blood–brain barrier
cART	Combination antiretroviral therapy
CNS	Central nervous system
ERK	Extracellular signal-regulated kinase
GFAP	Glial fibrillary acidic protein
HIV	Human immunodeficiency virus
IBA-1	Ionized calcium-binding adaptor molecule 1
MAPK	Mitogen-activated protein kinase
Meth	Methamphetamine
MMP-9	Matrix metalloproteinase-9
NF-κB	Nuclear factor-kappa B

REFERENCES

Abdulle S, Hagberg L, & Gisslén M (2005). Effects of antiretroviral treatment on blood-brain barrier integrity and intrathecal immunoglobulin production in neuroasymptomatic HIV-1-infected patients. HIV Med, 6, 164–169. 10.1111/j.1468-1293.2005.00281.x [PubMed: 15876282]

Andras IE, Pu H, Deli MA, Nath A, Hennig B, & Toborek M (2003). HIV-1 Tat protein alters tight junction protein expression and distribution in cultured brain endothelial cells. Journal of Neuroscience Research, 74, 255–265. 10.1002/jnr.10762 [PubMed: 14515355]

András IE, Pu H, Tian J, Deli MA, Nath A, Hennig B, & Toborek M (2005). Signaling mechanisms of HIV-1 Tat-induced alterations of claudin-5 expression in brain endothelial cells. Journal of Cerebral Blood Flow and Metabolism, 25, 1159–1170. 10.1038/sj.jcbfm.9600115 [PubMed: 15815581]

Anesten B, Yilmaz A, Hagberg L, Zetterberg H, Nilsson S, Brew BJ, … Gisslén M (2016). Blood-brain barrier integrity, intrathecal immunoactivation, and neuronal injury in HIV. Neurology - Neuroimmunology Neuroinflammation, 3, e300. 10.1212/NXI.0000000000000300 [PubMed: 27868081]

Arts EJ, & Hazuda DJ (2012). HIV-1 antiretroviral drug therapy. Cold Spring Harbor Perspectives in Medicine, 2(4), a007161. 10.1101/cshperspect.a007161 [PubMed: 22474613]

Ben HN, Leghmari K, Planes R, Thieblemont N, & Bahraoui E (2013). HIV-1 Tat protein binds to TLR4-MD2 and signals to induce TNF-alpha and IL-10. Retrovirology, 10, 123. [PubMed: 24165011]

Bloomfield PS, Bonsall D, Wells L, Dormann D, Howes O, & De Paola V (2018). The effects of haloperidol on microglial morphology and translocator protein levels: An in vivo study in rats using an automated cell evaluation pipeline. Journal of Psychopharmacology, 32, 1264–1272. 10.1177/0269881118788830 [PubMed: 30126329]

Bond M, Chase AJ, Baker AH, & Newby AC (2001). Inhibition of transcription factor NF-kappaB reduces matrix metalloproteinase-1, −3 and −9 production by vascular smooth muscle cells. Cardiovascular Research, 50, 556–565. [PubMed: 11376631]

Bradford MM (1976). A rapid and sensitive method for the quantification of microgram quantities of protein utilizing the principle of protein-dye binding. Analytical Biochemistry, 72, 248–254. [PubMed: 942051]

Brown CN, Fultz EK, Ferdousian S, Rogers S, Lustig E, Page A, … Szumlinski KK (2020). Transgenic analyses of homer2 function within nucleus accumbens subregions in the regulation of

Author Manuscript Author Manuscript Author Manuscript Author Manuscript

methamphetamine reward and reinforcement in mice. Frontiers in Psychiatry, 11, 11. [PubMed: 32116834]

Castelo JM, Sherman SJ, Courtney MG, Melrose RJ, & Stern CE (2006). Altered hippocampal-prefrontal activation in HIV patients during episodic memory encoding. Neurology, 66(11), 1688–1695. 10.1212/01.wnl.0000218305.09183.70 [PubMed: 16769942]

Chen B-P, Huang X-X, Dong D-M, Wu H, Zhu T-Q, & Wang B-F (2020). The role of NMDA receptors in rat propofol self-administration. BMC Anesthesiology, 20(1), 149. 10.1186/s12871-020-01056-0 [PubMed: 32539742]

Chiodi F, Sonnerborg A, Albert J, Gaines H, Norkrans G, Hagberg L, … Fenyo EM (1988). Human immunodeficiency virus infection of the brain. I. Virus isolation and detection of HIV specific antibodies in the cerebrospinal fluid of patients with varying clinical conditions. Journal of the Neurological Sciences, 85, 245–257. 10.1016/0022-510X(88)90184-0 [PubMed: 3210022]

Chiu PS, & Lai SC (2013). Matrix metalloproteinase-9 leads to claudin-5 degradation via the NF-kappaB pathway in BALB/c mice with eosinophilic meningoencephalitis caused by Angiostrongylus cantonensis. PLoS One, 8, e53370. [PubMed: 23505411]

Choi MR, Chun J-W, Kwak SM, Bang SH, Jin Y-B, Lee Y, … Kim D-J (2018). Effects of acute and chronic methamphetamine administration on cynomolgus monkey hippocampus structure and cellular transcriptome. Toxicology and Applied Pharmacology, 355, 68–79. 10.1016/j.taap.2018.05.031 [PubMed: 29802913]

Crews FT, & Vetreno RP (2016). Mechanisms of neuroimmune gene induction in alcoholism. Psychopharmacology (Berl), 233, 1543–1557. 10.1007/s00213-015-3906-1 [PubMed: 25787746]

Daneman R (2012). The blood-brain barrier in health and disease. Annals of Neurology, 72, 648–672. 10.1002/ana.23648 [PubMed: 23280789]

Davis LE, Hjelle BL, Miller VE, Palmer DL, Llewellyn AL, Merlin TL, … Wiley CA (1992). Early viral brain invasion in iatrogenic human immunodeficiency virus infection. Neurology, 42, 1736–1739. 10.1212/WNL.42.9.1736 [PubMed: 1513462]

Dawson TM, Gehlert DR, McCabe RT, Barnett A, & Wamsley JK (1986). D-1 dopamine receptors in the rat brain: A quantitative autoradiographic analysis. Journal of Neuroscience, 6(8), 2352–2365. [PubMed: 3528408]

El-Hage N, Bruce-Keller AJ, Yakovleva T, Bazov I, Bakalkin G, Knapp PE, & Hauser KF (2008). Morphine exacerbates HIV-1 Tat-induced cytokine production in astrocytes through convergent effects on [Ca(2+)](i). NF-kappaB Trafficking and Transcription.PLoS One, 3(12), e4093. [PubMed: 19116667]

Esposito G, Capoccia E, Gigli S, Pesce M, Bruzzese E, D'Alessandro A, … Sarnelli G (2017). HIV-1 Tat-induced diarrhea evokes an enteric glia-dependent neuroinflammatory response in the central nervous system. Scientific Reports, 7, 7735. [PubMed: 28798420]

Eugenin EA, Greco JM, Frases S, Nosanchuk JD, & Martinez LR (2013). Methamphetamine alters blood brain barrier protein expression in mice, facilitating central nervous system infection by neurotropic Cryptococcus neoformans. Journal of Infectious Diseases, 208, 699–704. 10.1093/infdis/jit117 [PubMed: 23532099]

Farhadian SF, Mistry H, Kirchwey T, Chiarella J, Calvi R, Chintanaphol M, … Spudich SS (2019). Markers of CNS injury in adults living with HIV with CSF HIV not detected vs detected <20 copies/ml. Open Forum Infectious Diseases, 6, ofz528. [PubMed: 31893212]

Fiume G, Vecchio E, De LA, Trimboli F, Palmieri C, Pisano A, … Quinto I (2012). Human immunodeficiency virus-1 Tat activates NF-kappaB via physical interaction with IkappaB-alpha and p65. Nucleic Acids Research, 40, 3548–3562. [PubMed: 22187158]

Fredriksson R, Sreedharan S, Nordenankar K, Alsiö J, Lindberg FA, Hutchinson A, … Schiöth HB (2019). The polyamine transporter Slc18b1(VPAT) is important for both short and long time memory and for regulation of polyamine content in the brain. PLoS Genetics, 15, e1008455. 10.1371/journal.pgen.1008455 [PubMed: 31800589]

Gobbele R, Reith W, & Block F (2000). Cerebral vasculitis as a concomitant neurological illness in Crohn's disease. Nervenarzt, 71, 299–304. [PubMed: 10795098]

Author Manuscript Author Manuscript Author Manuscript Author Manuscript

Gordon-Fennell AG, Will RG, Ramachandra V, Gordon-Fennell L, Dominguez JM, Zahm DS, & Marinelli M (2019). The lateral preoptic area: A novel regulator of reward seeking and neuronal activity in the ventral tegmental area. Frontiers of Neuroscience, 13, 1433.

Graves SM, Clark MJ, Traynor JR, Hu XT, & Napier TC (2015). Nucleus accumbens shell excitability is decreased by methamphetamine self-administration and increased by 5-HT receptor inverse agonism and agonism. Neuropharmacology, 89, 113–121. [PubMed: 25229719]

Gulbransen BD, & Sharkey KA (2012). Novel functional roles for enteric glia in the gastrointestinal tract. Nature Reviews Gastroenterology & Hepatology, 9, 625–632. 10.1038/nrgastro.2012.138 [PubMed: 22890111]

He C (1996). Molecular mechanism of transcriptional activation of human gelatinase B by proximal promoter. Cancer Letters, 106, 185–191. 10.1016/0304-3835(96)04318-2 [PubMed: 8844971]

Hinkin CH, Barclay TR, Castellon SA, Levine AJ, Durvasula RS, Marion SD, … Longshore D (2007). Drug use and medication adherence among HIV-1 infected individuals. AIDS and Behavior, 11, 185–194. 10.1007/s10461-006-9152-0 [PubMed: 16897351]

Hong S-I, Kang S, Chen J-F, & Choi D-S (2019). Indirect medium spiny neurons in the dorsomedial striatum regulate ethanol-containing conditioned reward seeking. Journal of Neuroscience, 39, 7206–7217. [PubMed: 31315945]

Hoogland ICM, Westhoff D, Engelen-Lee JY, Melief J, Valls SM, Houben-Weerts JHMP, … van de Beek D (2018). Microglial activation after systemic stimulation with lipopolysaccharide and Escherichia coli. Frontiers in Cellular Neuroscience, 12, 110. 10.3389/fncel.2018.00110 [PubMed: 29755322]

Huang W, Eum SY, Andras IE, Hennig B, & Toborek M (2009). PPARalpha and PPARgamma attenuate HIV-induced dysregulation of tight junction proteins by modulations of matrix metalloproteinase and proteasome activities. FASEB Journal, 23, 1596–1606. [PubMed: 19141539]

Jiao H, Wang Z, Liu Y, Wang P, & Xue Y (2011). Specific role of tight junction proteins claudin-5, occludin, and ZO-1 of the blood-brain barrier in a focal cerebral ischemic insult. Journal of Molecular Neuroscience, 44(2), 130–139. 10.1007/s12031-011-9496-4 [PubMed: 21318404]

Ju SM, Song HY, Lee JA, Lee SJ, Choi SY, & Park J (2009). Extracellular HIV-1 Tat up-regulates expression of matrix metalloproteinase-9 via a MAPK-NF-kappaB dependent pathway in human astrocytes. Experimental & Molecular Medicine, 41, 86–93. [PubMed: 19287189]

Kanmogne GD, Primeaux C, & Grammas P (2005). HIV-1 gp120 proteins alter tight junction protein expression and brain endothelial cell permeability: Implications for the pathogenesis of HIV-associated dementia. Journal of Neuropathology and Experimental Neurology, 64, 498–505. 10.1093/jnen/64.6.498 [PubMed: 15977641]

Kirkpatrick MG, Gunderson EW, Johanson CE, Levin FR, Foltin RW, & Hart CL (2012). Comparison of intranasal methamphetamine and d-amphetamine self-administration by humans. Addiction, 107, 783–791. 10.1111/j.1360-0443.2011.03706.x [PubMed: 22050030]

Kousik SM, Carvey PM, & Napier TC (2014). Methamphetamine self-administration results in persistent dopaminergic pathology: Implications for Parkinson's disease risk and reward-seeking. European Journal of Neuroscience, 40, 2707–2714. 10.1111/ejn.12628 [PubMed: 24890790]

Kousik SM, Graves SM, Napier TC, Zhao C, & Carvey PM (2011). Methamphetamine-induced vascular changes lead to striatal hypoxia and dopamine reduction. NeuroReport, 22, 923–928. 10.1097/WNR.0b013e32834d0bc8 [PubMed: 21979424]

Kousik SM, Napier TC, & Carvey PM (2012). The effects of psychostimulant drugs on blood brain barrier function and neuroinflammation. Frontiers in Pharmacology, 3, 121. 10.3389/fphar.2012.00121 [PubMed: 22754527]

Kozak W, Conn CA, & Kluger MJ (1994). Lipopolysaccharide induces fever and depresses locomotor activity in unrestrained mice. American Journal of Physiology, 266, R125–R135. 10.1152/ajpregu.1994.266.1.R125 [PubMed: 8304533]

Kruzich PJ, & Xi J (2006). Differences in extinction responding and reinstatement of methamphetamine-seeking behavior between Fischer 344 and Lewis rats. Pharmacology Biochemistry and Behavior, 83(3), 391–395. 10.1016/j.pbb.2006.02.021 [PubMed: 16574207]

Author Manuscript Author Manuscript Author Manuscript Author Manuscript

Lee DE, Reid WC, Ibrahim WG, Peterson KL, Lentz MR, Maric D, … Hammoud DA (2014). Imaging dopaminergic dysfunction as a surrogate marker of neuropathology in a small-animal model of HIV. Molecular Imaging, 13. 10.2310/7290.2014.00031

Lentz MR, Peterson KL, Ibrahim WG, Lee DE, Sarlls J, Lizak MJ, … Hammoud DA (2014). Diffusion tensor and volumetric magnetic resonance measures as biomarkers of brain damage in a small animal model of HIV. PLoS One, 9, e105752. 10.1371/journal.pone.0105752 [PubMed: 25144656]

Lively S, & Schlichter LC (2018). Microglia responses to pro-inflammatory stimuli (LPS, IFNγ + TNFα) and reprogramming by resolving cytokines. Molecular and Cellular Biology, 20, 4699–4707.

Louboutin JP, Agrawal L, Reyes BA, Van Bockstaele EJ, & Strayer DS (2010). HIV-1 gp120-induced injury to the blood-brain barrier: Role of metalloproteinases 2 and 9 and relationship to oxidative stress. Journal of Neuropathology and Experimental Neurology, 69, 801–816. 10.1097/NEN.0b013e3181e8c96f [PubMed: 20613638]

Lull ME, & Block ML (2010). Microglial activation and chronic neurodegeneration. Neurotherapeutics: the Journal of the American Society for Experimental NeuroTherapeutics, 7, 354–365. 10.1016/j.nurt.2010.05.014 [PubMed: 20880500]

Maki PM, Cohen MH, Weber K, Little DM, Fornelli D, Rubin LH, … Martin E (2009). Impairments in memory and hippocampal function in HIV-positive vs HIV-negative women: A preliminary study. Neurology, 72, 1661–1668. 10.1212/WNL.0b013e3181a55f65 [PubMed: 19433739]

Melega WP, Cho AK, Harvey D, & Lacan G (2007). Methamphetamine blood concentrations in human abusers: application to pharmacokinetic modeling. Synapse (New York, N. Y.), 61, 216–220. 10.1002/syn.20365 [PubMed: 17230548]

Mishra M, Flaga J, & Kowluru RA (2016). Molecular mechanism of transcriptional regulation of matrix metalloproteinase-9 in diabetic retinopathy. Journal of Cellular Physiology, 231, 1709–1718. 10.1002/jcp.25268 [PubMed: 26599598]

Moman RN, Gupta N, Sheikh NS, & Varacallo M (2020). Physiology, albumin. StatPearls Treasure Island, FL: StatPearls Publishing. https://www.ncbi.nlm.nih.gov/books/NBK459198/.

Mueller SG, Chao LL, Berman B, & Weiner MW (2011). Evidence for functional specialization of hippocampal subfields detected by MR subfield volumetry on high resolution images at 4 T. NeuroImage, 56(3), 851–857. [PubMed: 21419225]

Muradashvili N, Qipshidze N, Munjal C, Givvimani S, Benton RL, Roberts AM, … Lominadze D (2012). Fibrinogen-induced increased pial venular permeability in mice. Journal of Cerebral Blood Flow and Metabolism, 32(1), 150–163. 10.1038/jcbfm.2011.144 [PubMed: 21989482]

Nerlander LMC, Hoots BE, Bradley H, Broz D, Thorson A, & Paz-Bailey G (2018). HIV infection among MSM who inject methamphetamine in 8 US cities. Drug and Alcohol Dependence, 190, 216–223. 10.1016/j.drugalcdep.2018.06.017 [PubMed: 30055426]

Northrop NA, Halpin LE, & Yamamoto BK (2016). Peripheral ammonia and blood brain barrier structure and function after methamphetamine. Neuropharmacology, 107, 18–26. 10.1016/j.neuropharm.2016.03.018 [PubMed: 26972828]

Ohene-Nyako M, Persons AL, & Napier TC (2018). Region-specific changes in markers of neuroplasticity revealed in HIV-1 transgenic rats by low dose methamphetamine. Brain Structure and Function, 223, 3503–3513. 10.1007/s00429-018-1701-6 [PubMed: 29931627]

Oliva I, & Wanat MJ (2019). Operant costs modulate dopamine release to self-administered cocaine. Journal of Neuroscience, 39, 1249–1260. [PubMed: 30559149]

Park JH, Seo YH, Jang JH, Jeong CH, Lee S, & Park B (2017). Asiatic acid attenuates methamphetamine-induced neuroinflammation and neurotoxicity through blocking of NF-kB/STAT3/ERK and mitochondria-mediated apoptosis pathway. Journal of Neuroinflammation, 14(1), 240. 10.1186/s12974-017-1009-0 [PubMed: 29228978]

Patel S, Leibrand CR, Palasuberniam P, Couraud P-O, Weksler B, Jahr FM, … McRae M (2017). Effects of HIV-1 Tat and methamphetamine on blood-brain barrier integrity and function in vitro. Antimicrobial Agents and Chemotherapy, 61(12), e01307–e1317. [PubMed: 28893794]

Paxinos G, & Watson C (2009). The rat brain in stereotaxic coordinates Compact 6th ed. Academic Press.

Author Manuscript Author Manuscript Author Manuscript Author Manuscript

Peng J, Vigorito M, Liu X, Zhou D, Wu X, & Chang SL (2010). The HIV-1 transgenic rat as a model for HIV-1 infected individuals on HAART. Journal of Neuroimmunology, 218, 94–101. 10.1016/j.jneuroim.2009.09.014 [PubMed: 19913921]

Persons AL, Bradaric BD, Dodiya HB, Ohene-Nyako M, Forsyth CB, Keshavarzian A, … Napier TC (2018). Colon dysregulation in methamphetamine self-administering HIV-1 transgenic rats. PLoS One, 13, e0190078. 10.1371/journal.pone.0190078 [PubMed: 29293553]

Rahimy E, Li F-Y, Hagberg L, Fuchs D, Robertson K, Meyerhoff DJ, … Spudich S (2017). Blood-brain barrier disruption is initiated during primary HIV infection and not rapidly altered by antiretroviral therapy. Journal of Infectious Diseases, 215, 1132–1140. 10.1093/infdis/jix013 [PubMed: 28368497]

Reid WC, Ibrahim WG, Kim SJ, Denaro F, Casas R, Lee DE, … Hammoud DA (2016). Characterization of neuropathology in the HIV-1 transgenic rat at different ages. Journal of Neuroimmunology, 292, 116–125. 10.1016/j.jneuroim.2016.01.022 [PubMed: 26943969]

Repunte-Canonigo V, Lefebvre C, George O, Kawamura T, Morales M, Koob GF, … Sanna PP (2014). Gene expression changes consistent with neuroAIDS and impaired working memory in HIV-1 transgenic rats. Molecular Neurodegeneration, 9, 26. [PubMed: 24980976]

Resnick L, Berger JR, Shapshak P, & Tourtellotte WW (1988). Early penetration of the blood-brain-barrier by HIV. Neurology, 38, 9–14. 10.1212/WNL.38.1.9

Soontornniyomkij V, Kesby JP, Morgan EE, Bischoff-Grethe A, Minassian A, Brown GG, & Grant I (2016). Effects of HIV and methamphetamine on brain and behavior: Evidence from human studies and animal models. Journal of Neuroimmune Pharmacology: the Official Journal of the Society on NeuroImmune Pharmacology, 11, 495–510. 10.1007/s11481-016-9699-0 [PubMed: 27484318]

Sugaya-Fukasawa M, Watanabe T, Tamura M, Egashira S, & Hisatomi H (2011). Glial fibrillary acidic protein is one of the key factors underlying neuron-like elongation in PC12 cells. Experimental and Therapeutic Medicine, 2(1), 85–87. 10.3892/etm.2010.162 [PubMed: 22977474]

Toschi E, Bacigalupo I, Strippoli R, Chiozzini C, Cereseto A, Falchi M, … Ensoli B (2006). HIV-1 Tat regulates endothelial cell cycle progression via activation of the Ras/ERK MAPK signaling pathway. Molecular Biology of the Cell, 17, 1985–1994. [PubMed: 16436505]

Uhlen M, Bandrowski A, Carr S, Edwards A, Ellenberg J, Lundberg E, … Yamamoto T (2016). A proposal for validation of antibodies. Nature Methods, 13, 823–827. 10.1038/nmeth.3995 [PubMed: 27595404]

Valjent E, Pascoli V, Svenningsson P, Paul S, Enslen H, Corvol JC et al. (2005). Regulation of a protein phosphatase cascade allows convergent dopamine and glutamate signals to activate ERK in the striatum. Proceedings of the National Academy of Sciences of the United States of America, 102, 491–496. [PubMed: 15608059]

Vermeer PD, Denker J, Estin M, Moninger TO, Keshavjee S, Karp P, … Zabner J (2009). MMP9 modulates tight junction integrity and cell viability in human airway epithelia. American Journal of Physiology. Lung Cellular and Molecular Physiology, 296, L751–L762. 10.1152/ajplung.90578.2008 [PubMed: 19270179]

Wang X, Northcutt AL, Cochran TA, Zhang X, Fabisiak TJ, Haas ME, … Watkins LR (2019). Methamphetamine activates toll-like receptor 4 to induce central immune signaling within the ventral tegmental area and contributes to extracellular dopamine increase in the nucleus accumbens shell. ACS Chemical Neuroscience, 10(8), 3622–3634. 10.1021/acschemneuro.9b00225 [PubMed: 31282647]

Watkins S, Robel S, Kimbrough IF, Robert SM, Ellis-Davies G, & Sontheimer H (2014). Disruption of astrocyte-vascular coupling and the blood-brain barrier by invading glioma cells. Nature Communications, 5, 4196. 10.1038/ncomms5196

Xu R, Feng X, Xie X, Zhang J, Wu D, & Xu L (2012). HIV-1 Tat protein increases the permeability of brain endothelial cells by both inhibiting occludin expression and cleaving occludin via matrix metalloproteinase-9. Brain Research, 1436, 13–19. 10.1016/j.brainres.2011.11.052 [PubMed: 22197032]

Yang Y, Estrada EY, Thompson JF, Liu W, & Rosenberg GA (2007). Matrix metalloproteinase-mediated disruption of tight junction proteins in cerebral vessels is reversed by synthetic

Author Manuscript Author Manuscript Author Manuscript Author Manuscript

matrix metalloproteinase inhibitor in focal ischemia in rat. Journal of Cerebral Blood Flow and Metabolism, 27, 697–709. 10.1038/sj.jcbfm.9600375 [PubMed: 16850029]

Yu YB, & Li YQ (2014). Enteric glial cells and their role in the intestinal epithelial barrier. World Journal of Gastroenterology, 20, 11273–11280. 10.3748/wjg.v20.i32.11273 [PubMed: 25170211]

Zhang Y, Zhu T, Zhang X, Chao J, Hu G, & Yao H (2015). Role of high-mobility group box 1 in methamphetamine-induced activation and migration of astrocytes. Journal of Neuroinflammation, 12, 156. 10.1186/s12974-015-0374-9 [PubMed: 26337661]

Author Manuscript Author Manuscript Author Manuscript Author Manuscript

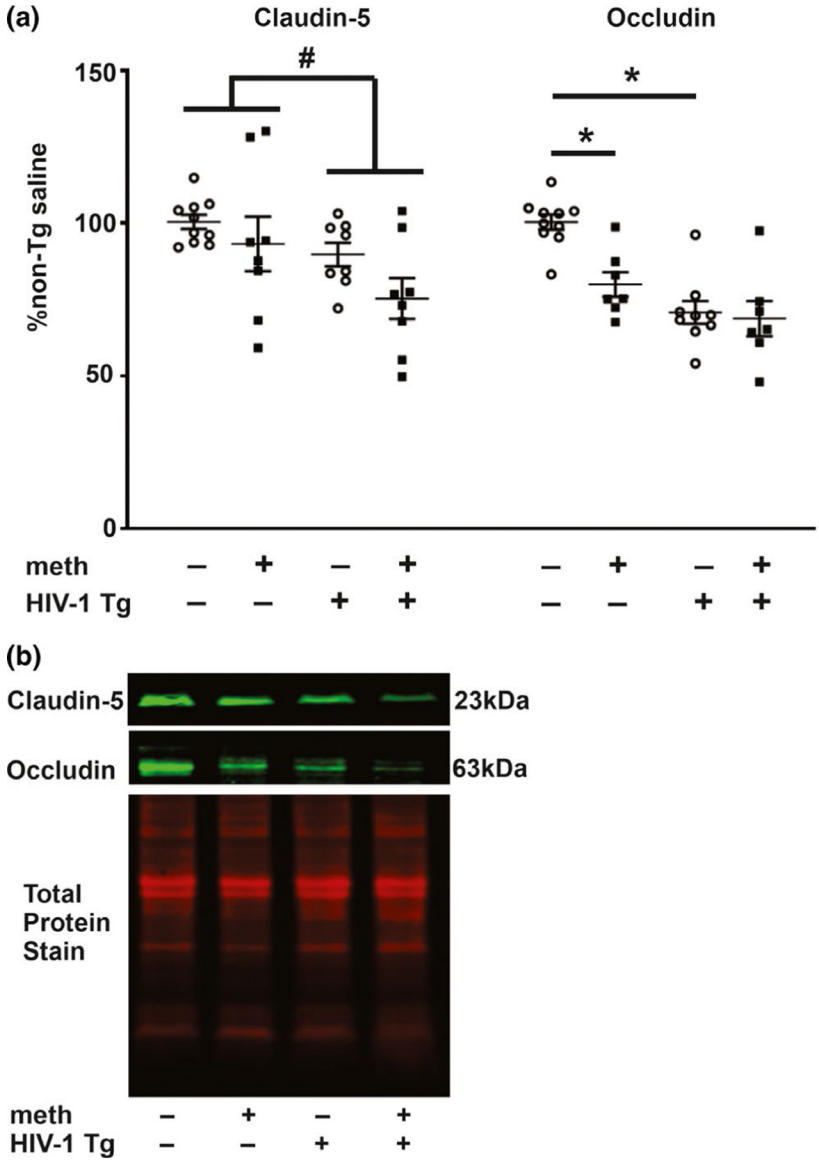

FIGURE 1.

Claudin-5 and occludin protein levels. (a) Claudin-5 levels were reduced in the hippocampus of HIV-1 Tg rats irrespective of treatment. Occludin levels were also reduced independently by the HIV-1 transgene and by meth. (b) Representative photomicrograph of claudin-5, occludin and total protein immunoblots. Data are expressed as mean + *SEM*. # indicates significant main effects by two-way ANOVA. * indicates planned contrasts that showed differences with a Newman–Keuls *post hoc* test ($p < .05$). Cldn-5, claudin-5; occldn, occludin. $n = 8$/group [Colour figure can be viewed at wileyonlinelibrary.com]

Author Manuscript Author Manuscript Author Manuscript Author Manuscript

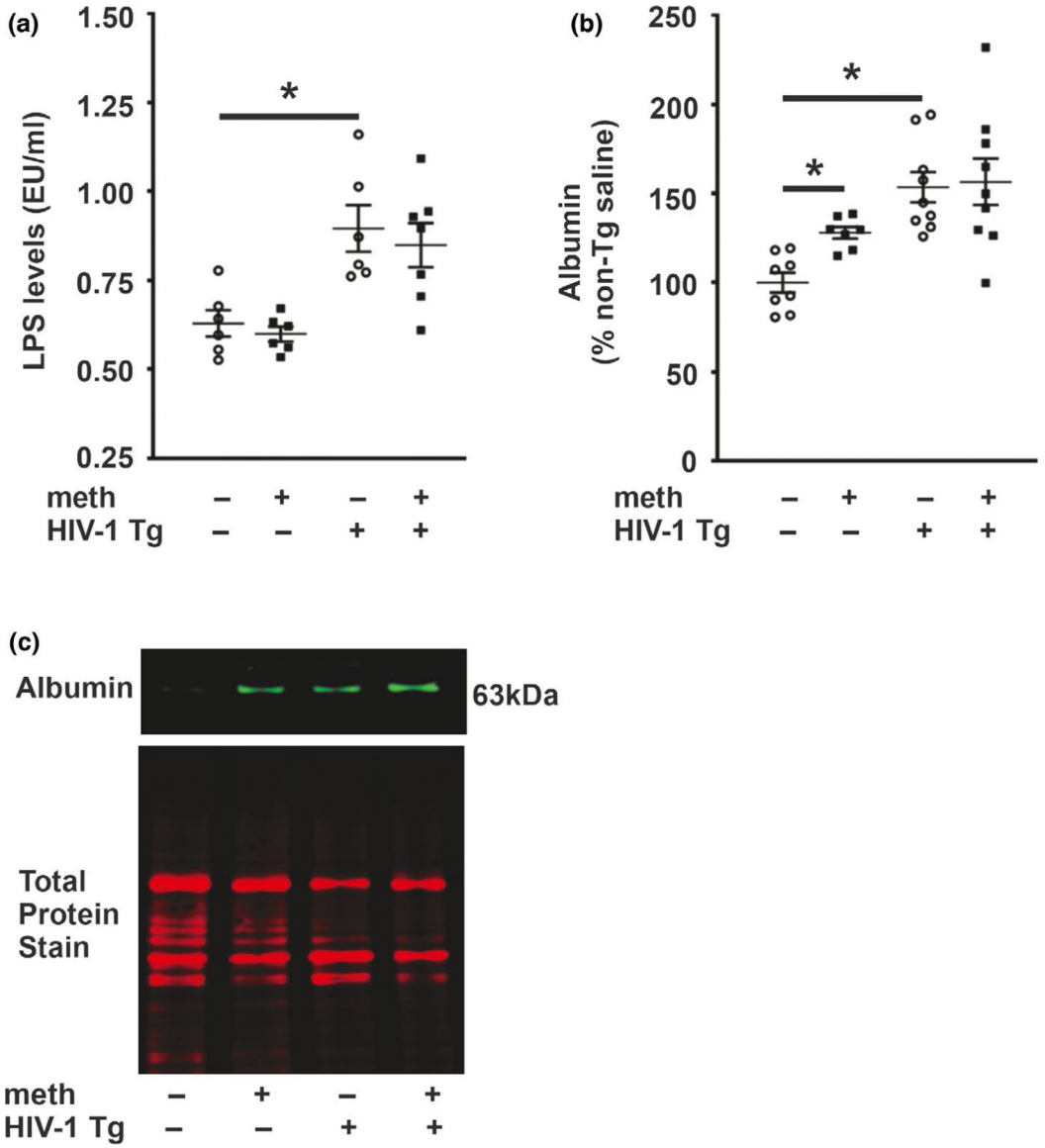

FIGURE 2.

Lipopolysaccharide concentrations and albumin level. (a) Lipopolysaccharide concentration was increased in HIV-1 Tg rats irrespective of treatment. (b) Albumin level was increased in HIV-1 Tg rats and meth self-administering non-Tg rats. (c) Representative photomicrograph of albumin and total protein immunoblots. Data are expressed as mean + *SEM*. * indicates planned contrasts that showed differences with a Newman–Keuls *post hoc* test ($p < .05$). EU, endotoxin unit; LPS, lipopolysaccharide. $n = 6–9$/group [Colour figure can be viewed at wileyonlinelibrary. com]

Author Manuscript Author Manuscript Author Manuscript Author Manuscript

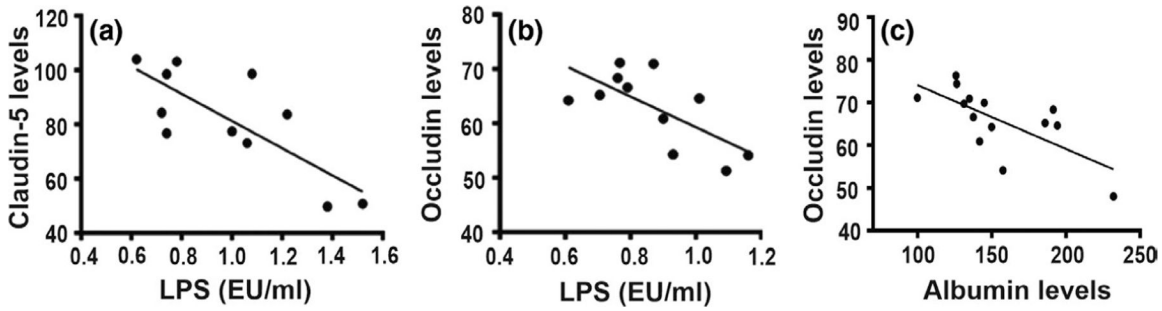

FIGURE 3.

Correlation of tight junction protein levels and BBB functional integrity markers. Pearson's correlation revealed that tight junction protein levels in HIV-1 Tg rats (pooled across treatments) negatively correlated with lipopolysaccharide levels (a and b) and albumin level (c) ($p < .05$). EU, endotoxin unit; LPS, lipopolysaccharide

Author Manuscript Author Manuscript Author Manuscript Author Manuscript

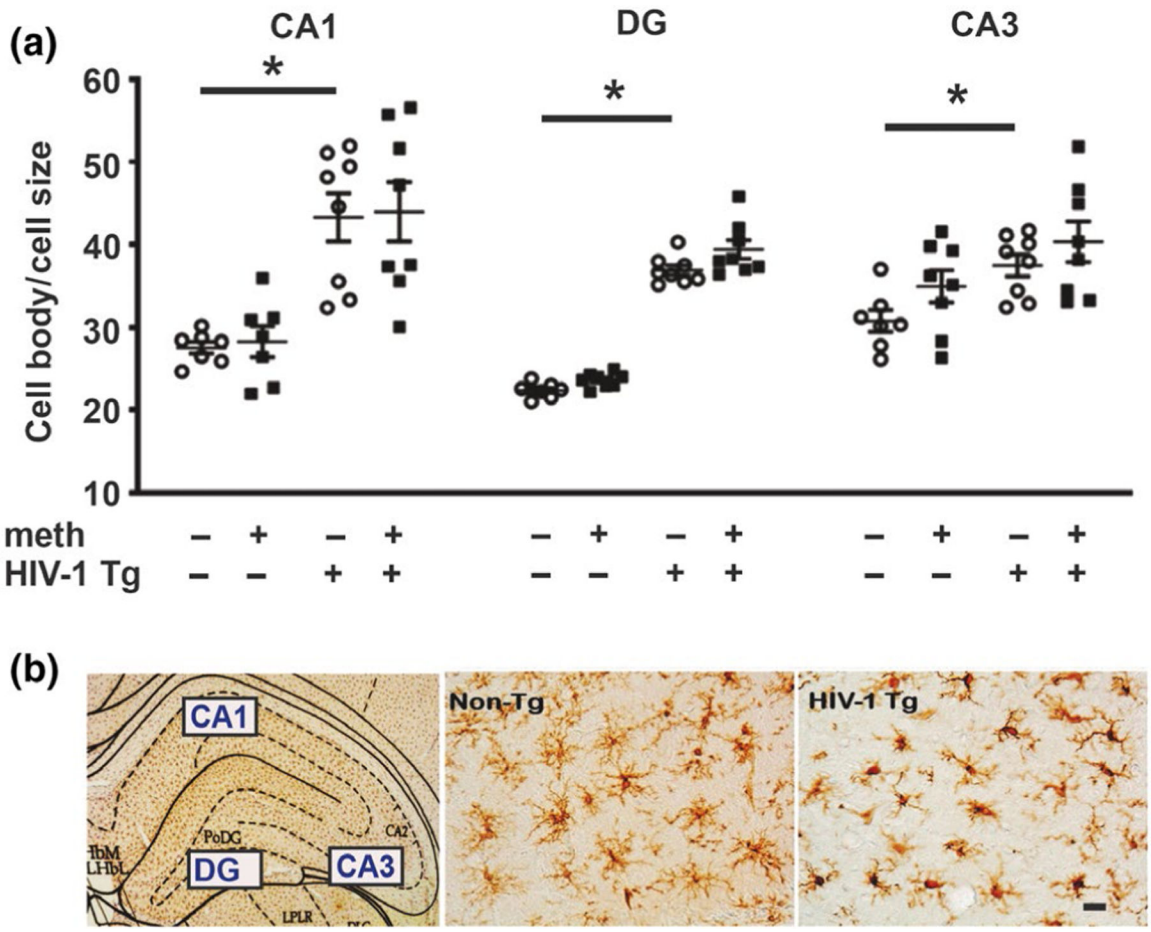

FIGURE 4.

Iba-1-stained microglia. (a) Increased cell body/cell size ratios of Iba-1-stained microglia were observed in all three subfields of the hippocampus in HIV-1 Tg rats. (b) Photomicrograph (5x) showing the evaluated subfields of the hippocampus and 40x photomicrographs showing increased microglial cell body and retracted processes in HIV-1 Tg rats versus smaller cell body sizes with long ramifications in dentate gyrus of non-Tg rats. Scale bar: 10μm. Data are expressed as mean + *SEM*. * indicates planned contrasts that showed differences with a Newman–Keuls *post hoc* test ($p < .05$). CA, cornu ammonis; DG, dentate. $n = 8$/group [Colour figure can be viewed at wileyonlinelibrary.com]

Author Manuscript Author Manuscript Author Manuscript Author Manuscript

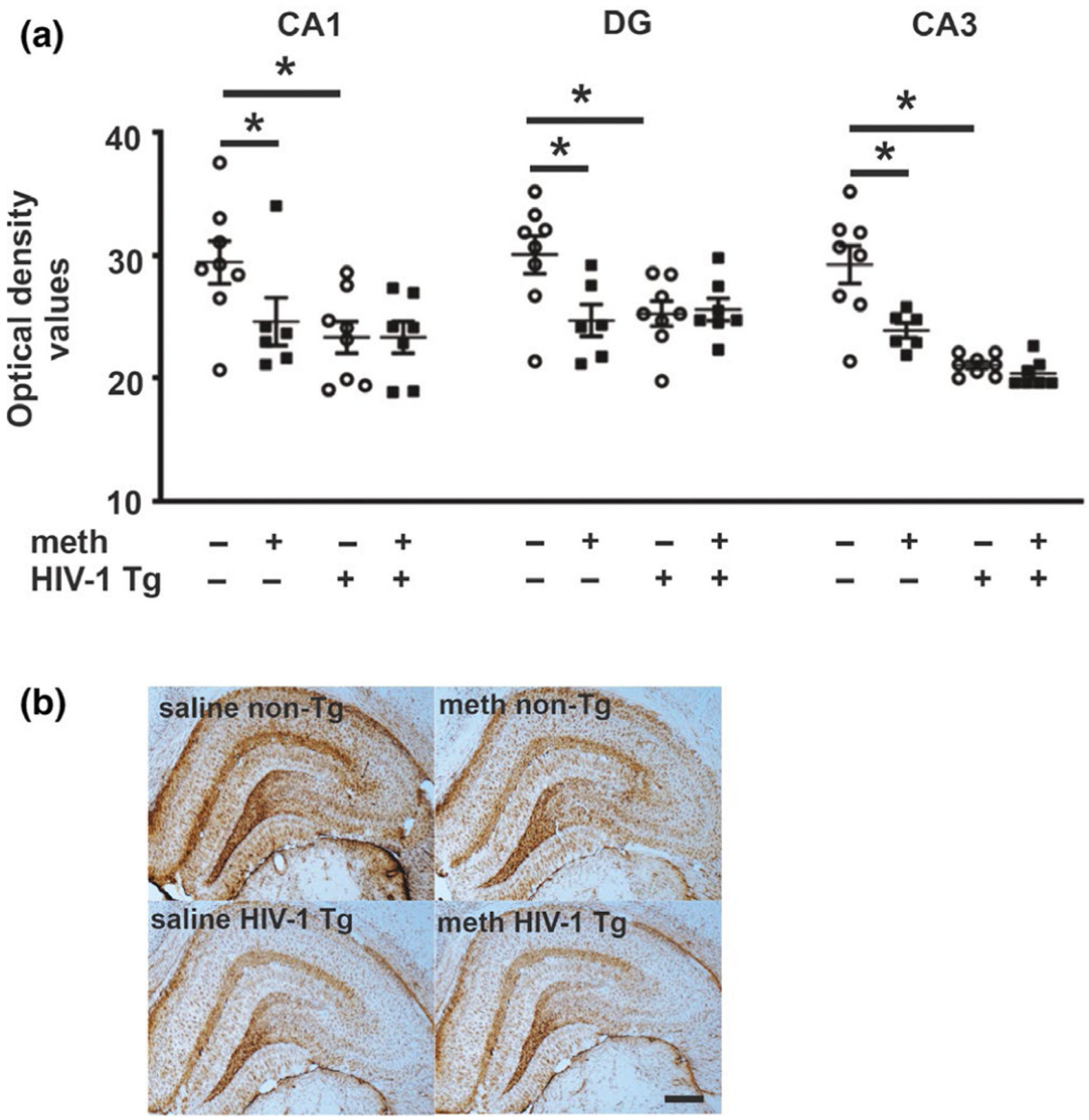

FIGURE 5.

GFAP-stained astroglia. (a) GFAP immunoreactivity was decreased independently by the presence of the HIV-1 transgene and by meth in all evaluated hippocampal subfields. (b) Photomicrograph (5X) of GFAP staining in hippocampus of Tg and non-Tg rats. Scale bar: 200μm. Data are expressed as mean + *SEM*. * indicates planned contrasts that showed differences with a Newman–Keuls *post hoc* test ($p < .05$). CA, cornu ammonis; DG, dentate. $n = 8$/group [Colour figure can be viewed at wileyonlinelibrary.com]

Author Manuscript Author Manuscript Author Manuscript Author Manuscript

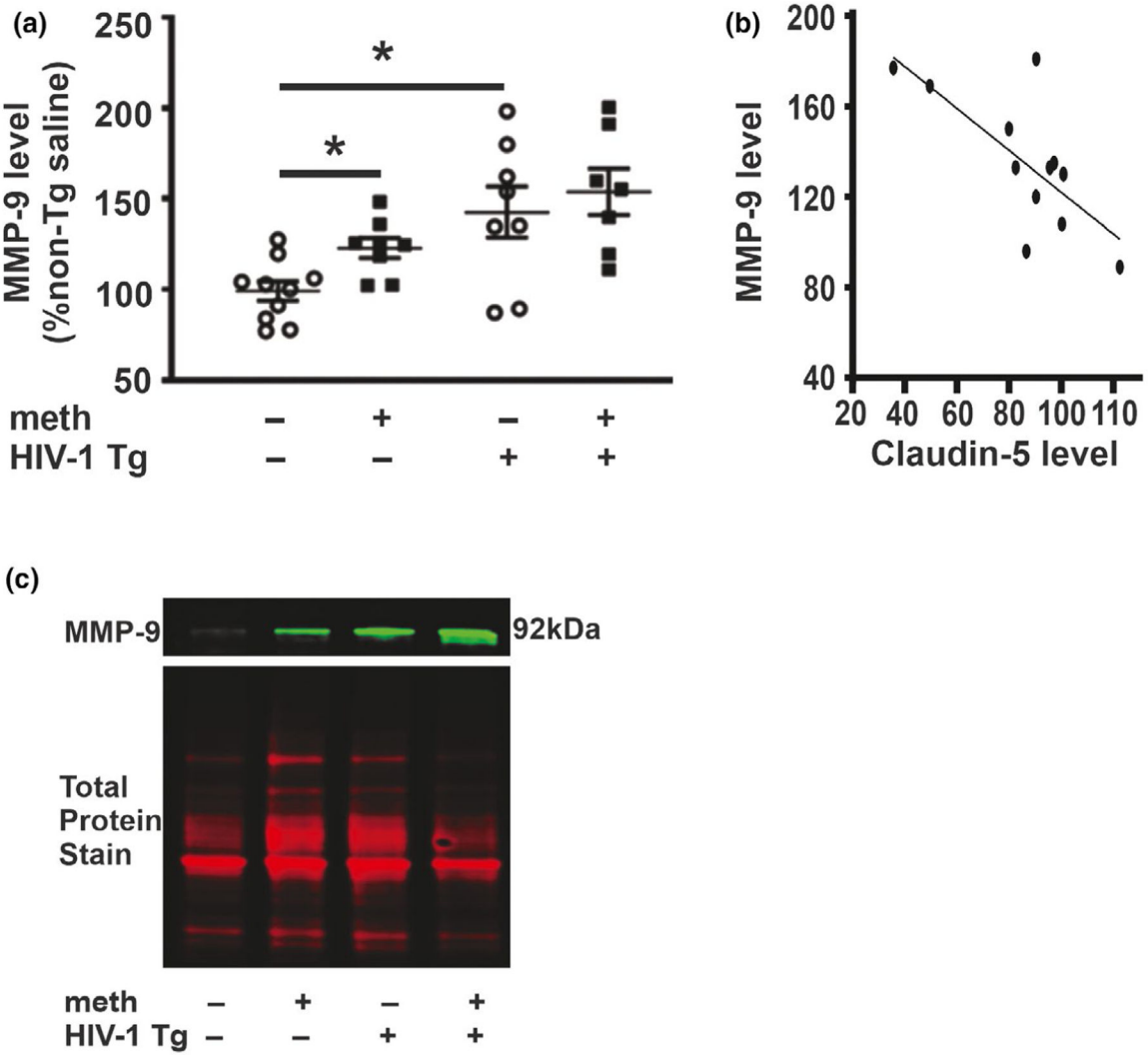

FIGURE 6.

MMP-9 protein levels. (a) MMP-9 protein levels were increased independently by the HIV-1 transgene and by meth. (b) Pearson's correlation revealed that level of claudin-5 in HIV-1 Tg rats (pooled across treatments) negatively correlated with level of MMP-9. (c) Representative photomicrograph of immunoblots showing MMP-9-like bands (top) and total protein (bottom). Data are expressed as mean + *SEM*. * indicates planned contrasts that showed differences with a Newman–Keuls *post hoc* test ($p < .05$). $n = 8$/group [Colour figure can be viewed at wileyonlinelibrary.com]

Author Manuscript Author Manuscript Author Manuscript Author Manuscript

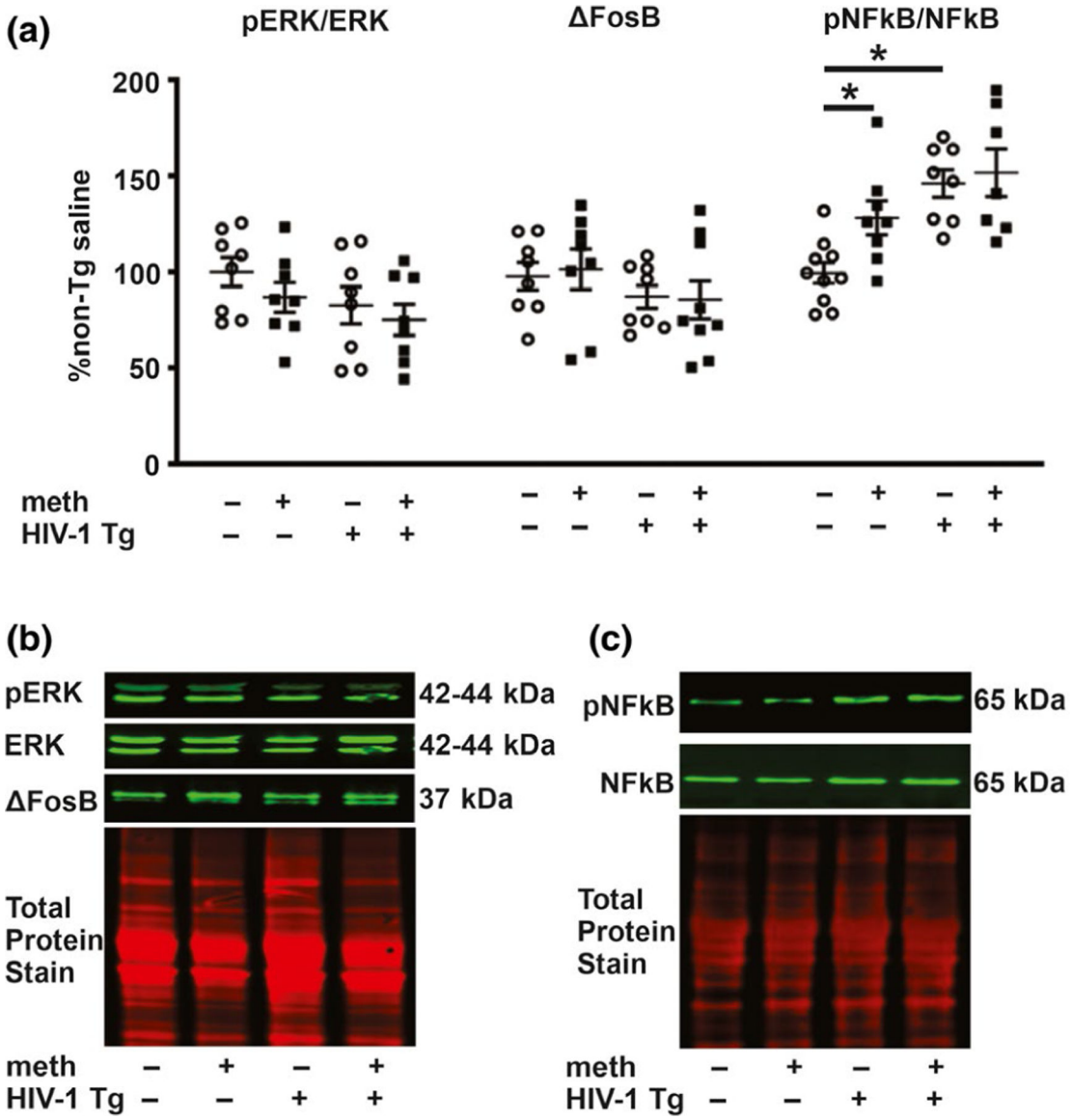

FIGURE 7.

ERK, ΔFosB and NF-κB protein levels. (a) There were no significant differences in any of the evaluated groups for ERK and ΔFosB levels by two-way ANOVA. pNF-κB/NF-κB levels were increased independently by the HIV-1 transgene and by meth. (b) Representative photomicrographs of immunoblots for pERK, ERK and ΔFosB, and the total protein. (c) Representative photomicrographs of immunoblots for pNF-κB and NF-κB. Data are expressed as mean + *SEM*. * indicates planned contrasts that showed differences with a Newman–Keuls *post hoc* test ($p < .05$). $n = 7–8$/group [Colour figure can be viewed at wileyonlinelibrary.com]